

Spatio-temporal synchronization of recurrent epidemics

Daihai He and Lewi Stone*

Biomathematics Unit, Department of Zoology, Tel Aviv University, Ramat Aviv, Tel Aviv 69978, Israel

Long-term spatio-temporal datasets of disease incidences have made it clear that many recurring epidemics, especially childhood infections, tend to synchronize in-phase across suburbs. In some special cases, epidemics between suburbs have been found to oscillate in an out-of-phase ('antiphase') relationship for lengthy periods. Here, we use modelling techniques to help explain the presence of in-phase and antiphase synchronization. The nonlinearity of the epidemic dynamics is often such that the intensity of the outbreak influences the phase of the oscillation thereby introducing 'shear', a factor that is found to be important for generating antiphase synchronization. By contrast, the coupling between suburbs via the immigration of infectives tends to enhance in-phase synchronization. The emerging synchronization depends delicately on these opposite factors. We use theoretical results from continuous time models to provide a framework for understanding the relationship between synchronization patterns for different model structures.

Keywords: epidemics; epidemic models; synchronization; antiphase; shear; vaccination strategies

1. INTRODUCTION

The number of newly emerging pathogens and re-emerging infectious diseases has increased alarmingly over the past decades in what has been likened to an 'epidemic of epidemics' (Karlen 1995). Many such diseases are widespread and occur across the globe, the more established ones often manifesting themselves in the form of recurrent epidemics. Some, especially childhood infectious diseases, might best be classified as periodic cycles with deviations arising from stochastic effects, or possibly even influenced to some degree by chaotic dynamics (Anderson *et al.* 1984; Anderson & May 1991; Rohani *et al.* 2002). For example, chickenpox is often seen as an annual cycle, measles is often characterized by an underlying 2 year biennial cycle (see figure 1), although arguably chaotic, and whooping cough recurs roughly every 3–4 years. One of our main goals is to study the manner in which two or more communities or suburbs synchronize in time, as recurring waves of infection sweep through their respective populations. This is a fascinating outcome of spatial dynamics whereby a few migrating infective individuals have the potential to spread the epidemic from one community to the other, giving rise to synchrony in the long term. Figure 1, for example shows time-series of measles infections in various cities of England (1944–1958); Birmingham and Newcastle appear to synchronize in-phase together while Cambridge and Norwich are clearly out of phase by 180° (Grenfell *et al.* 2001). We term the 180° out-of-phase synchronization 'antiphase'. Using a seasonally forced epidemic model, Grenfell *et al.* (2001) noted coexisting in-phase and antiphase attractors that reproduced this behaviour. But apart from Lloyd & May (1996) there are very few theoretical works explaining the synchronization patterns of epidemics, and most are usually only devoted to the study of in-phase synchronization.

Currently, there is very little understanding of the factors that lead to more complex forms of synchronization, such as the antiphase patterns observed between Cambridge and Norwich. Here, we analyse simple coupled epidemiological models to gain deeper insights. This is all the more important, given that the spatial synchronization of epidemics is believed to be a key factor affecting their long-term patterns of persistence and extinction (Earn *et al.* 1998).

We require an epidemiological model that is capable of generating sustained oscillations and yet simple enough to analyse mathematically. Seasonally forced epidemic models are avoided for two reasons. First, the model equations of a coupled system tend to become analytically intractable, making it almost impossible to gain theoretical insights into any raw synchronization mechanisms. Second, epidemics often oscillate at their own intrinsic time-scales. The period of the oscillations is usually distinctive of the disease, dependent on its virulence and transmission rates (Anderson & May 1991). Thus, the oscillations we seek to model are often determined by the disease itself.

Alternatively, the conventional unforced deterministic epidemic models (usually systems of mean-field differential equations) are unable to generate sustained oscillations without further sophistication such as the incorporation of time delays (Hethcote & Levin 1989). Stochastic formulations are sometimes resorted to whereby noise forcing prevents the system from ever attaining equilibrium, thereby maintaining damped oscillations. Neither of these alternative types of model is well suited for the study of complex synchronization patterns, since the problem becomes mathematically intractable (see Keeling & Rohani (2002) for the in-phase case).

We have, therefore, chosen to use a discrete-time formulation of the classical 'SIRS' epidemic model which simulates an infectious disease as it spreads through a population, and has a known propensity to oscillate (Cooke *et al.* 1977; Kuperman & Abramson 2001; Girvan

* Author for correspondence (zoology@ccsg.tau.ac.il).

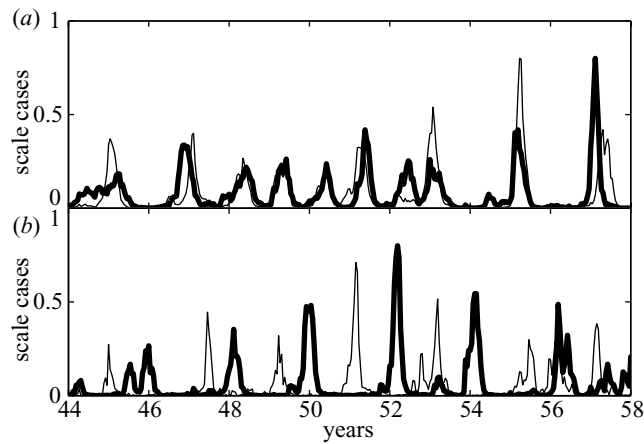


Figure 1. Weekly measles case reports for Birmingham, Newcastle, Cambridge and Norwich between 1944 and 1958. (a) In-phase synchronized pattern of weekly case reports between Birmingham (thin line) and Newcastle (bold line); (b) antiphase pattern of weekly case reports between Cambridge (thin line) and Norwich (bold line). Data made available by Professor B. T. Grenfell.

et al. 2002). At any time an individual can belong to one of three classes: susceptible (S), infected (I) and recovered (R). Movement between the classes is governed by the following rules.

- (i) Susceptibles pass to the infected state after coming into contact with an infected individual.
- (ii) Infected individuals pass to the recovered state after a fixed period τ_I has elapsed since the time of infection.
- (iii) Recovered elements return to the susceptible state after a recovery time τ_R , and the $S \rightarrow I \rightarrow R \rightarrow S$ 'cycle' is complete.

Thus, even though individuals become infected by the disease, they eventually lose immunity (referred to as waning immunity) and can be reinfected once again. If τ_R is infinitely long we retrieve the SIR model. The recovery and return of individuals to the susceptible population is one of the features promoting oscillatory behaviour. The SIRS formulation is most appropriate for bacterial diseases such as gonorrhoea, meningitis and streptococcal sore throat, and is a useful model for exploring ideas concerning antibiotic resistance (Hethcote & Levin 1989; Girvan *et al.* 2002). Note that a discrete-time SIR model with vital dynamics (birth and death rates) is also able to generate similar oscillations, and is perhaps more appropriate for diseases such as childhood infections (measles, mumps, chickenpox) which induce immunity. But since we are more concerned with the mechanism behind spatial synchronization, we prefer to stay with the simplest model formulation.

2. EPIDEMIC SYNCHRONIZATION IN COUPLED NETWORKS

The model is easily cast in a simulation framework. Consider a population of N individuals. The population can be treated as a graph with each node representing an individual, and each link in the graph representing a con-

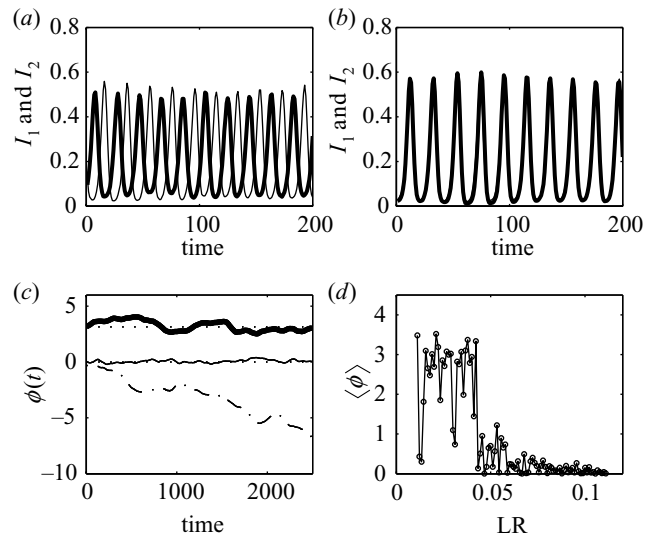


Figure 2. The infected fraction of sites in two coupled random networks. (a) With weak coupling, $LR \approx 0.01$, antiphase synchronization predominates. (b) With strong coupling, $LR \approx 0.1$, the two populations synchronize in-phase. (c) The phase difference $\phi(t) = \theta_1(t) - \theta_2(t)$ between two infected fractions $I_{1,2}$ versus time. The solid curve fluctuating close to $\phi = 0$ corresponds to in-phase synchronization ($LR = 0.1$, i.e. high coupling between networks). The bold curve fluctuating close to $\phi = \pi$ corresponds to antiphase synchronization ($LR = 0.01$, i.e. weak coupling between networks). The dashed curve portrays the phase difference between two networks without any coupling. (d) The time average phase difference $\langle \phi \rangle = \langle \theta_1 - \theta_2 \rangle$ between two infected fractions $I_{1,2}$ as a function of the LR. The abrupt change from antiphase to in-phase synchronization between the two communities occurs when $LR \approx 0.04$.

nection between two individuals through which an infection may potentially be transmitted. Connected pairs of individuals are referred to as neighbours. Links are added between nodes randomly so that on average each node is connected to k neighbours. This network structure requires randomly connecting $kN/2$ pairs of individuals. We term this the number of intra-links in the community.

Disease contagion is modelled as follows. Suppose node i is in the susceptible state and has k_i neighbours, of which k_{inf} are infected. The probability that node i becomes infected at a given time-step is taken to be $\lambda_1 = k_{inf}/k_i$. Observe that the node will become infected with probability $\lambda_1 = 1$ if all its neighbours are infected. Other contagion schemes are also possible, but change little the basic results reported below. For example, let q be the probability that an infected neighbour successfully infects a susceptible. The probability of a susceptible node becoming infected could then be reasonably modelled as $\lambda_2 = [1 - (1 - q)^{k_{inf}}]$ (Kuperman & Abramson 2001).

The SIRS network model generates oscillations over a large parameter range. Figure 2a,b gives the time-series of a typical model run. For this example, $N = 3000$ nodes with on average $k = 6$ links per node, infective period $\tau_I = 4$ and the recovery period $\tau_R = 9$. The infected fraction I of the network exhibits an oscillation with mean period about 20 time-units, which is, as expected, slightly larger than $2\tau_R$ (see Kuperman & Abramson 2001).

Consider now, two such networks, each representing a community or suburb, and suppose a small number of infective individuals pass from one community to the other. This might be modelled by randomly connecting *inter-links* between the two networks. The strength of coupling between the two communities is measured by

$$\text{LR} = \text{links ratio} = \frac{\text{no. of inter-links}}{\text{no. of intra-links}} \quad (2.1)$$

Although the approach is only a crude approximation of the dynamic nature of interactions between two communities, it nevertheless captures some of the essential elements. Figure 2a shows a simulation with relatively weak coupling between two populations. The infectives in each community are seen to oscillate in antiphase. Upon increasing the coupling strength (i.e. LR) between the communities, the suburbs show in-phase synchronization (see figure 2b).

The synchronization can be quantified by calculating the phase θ of each time-series of infectives and plotting the phase difference between the two suburbs. The phase of a time-series is defined as follows (Pikovsky *et al.* 2001):

$$\theta(t) = 2\pi \frac{t - \tau_k}{\tau_{k+1} - \tau_k} + 2\pi k, \quad (2.2)$$

where $\tau_k \leq t \leq \tau_{k+1}$ and τ_k is the time of the k th maximum of the time-series. When the two communities are synchronized, the phase difference $\phi(t) = \theta_1(t) - \theta_2(t)$ between them should be relatively constant with $\phi = 0$ for in-phase synchronization and $\phi = \pi$ for antiphase synchronization. Owing to stochastic effects the phase difference is likely to hover about these values rather than maintaining a strict equality. Figure 2c plots ϕ for three different coupling levels. When there is no coupling ϕ appears to decrease as the phase difference accumulates through random drift. For relatively weak coupling ϕ hovers close to the horizontal line $\phi = \pi$ indicating antiphase synchronization. However, for stronger coupling $\phi \approx 0$ indicating in-phase synchronization.

Figure 2d plots the mean phase difference $\langle \phi \rangle = \langle \theta_1 - \theta_2 \rangle$ as a function of the coupling between the two random networks. Each point on the graph represents the results of a single simulation ($N = 3000, k = 6$) at the given LR. It can be seen that there is a critical point at approximately $\text{LR} = 0.04$, below which most simulations (circles in figure 2d) are characterized by antiphase synchronization ($\langle \phi \rangle \approx \pi$) and above which they are mainly in-phase ($\langle \phi \rangle \approx 0$).

3. EPIDEMIC SYNCHRONIZATION OF COUPLED MAP SYSTEMS

The synchronization properties discussed in § 2 successfully mimic the pattern seen in the observed epidemic data (figure 1). We proceed to model the coupled communities by approximating the average behaviour of the SIRS network using a discrete-time model based on Cooke *et al.* (1977) and Girvan *et al.* (2002). As before, assume a constant closed population with no births or deaths. To keep things simple, suppose that susceptible individuals upon infection, spend one time-step in the infective class ($\tau_I = 1$), and a subsequent $\tau - 1$ time-steps in the immune

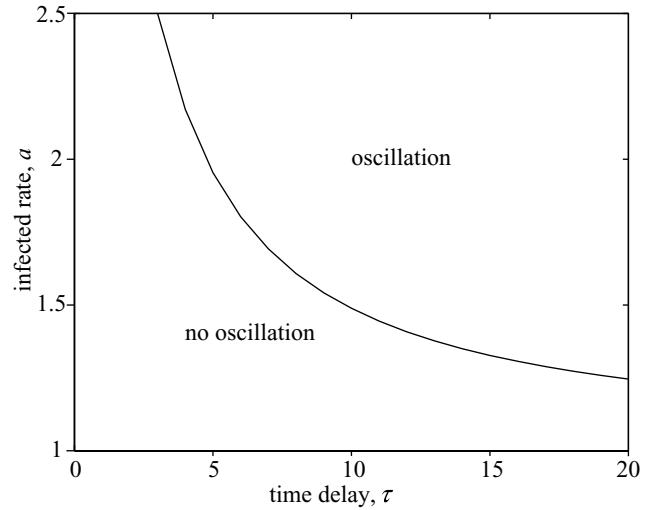


Figure 3. Hopf (Neimark) bifurcation curve for system (3.2).

class ($\tau_R = \tau - 1$). After these $\tau = \tau_I + \tau_R$ time-steps, individuals then return to the susceptible pool. Let x_t be the probability that an individual is infected at time t . The fraction of the population that is immune at any given time t , can be determined by examining the fraction which has been infected in any of the previous $\tau - 1$ time-steps. The proportion of the population that is susceptible (s_t) is simply the probability of being neither infected nor immune, i.e.

$$s_t = 1 - \sum_{k=0}^{\tau-1} x_{t-k}. \quad (3.1)$$

The fraction of infected individuals at time $t + 1$, is proportional to the number of susceptibles coming into contact with infectives. Assuming homogeneous mixing, this can be expressed as

$$x_{t+1} = ax_t s_t = ax_t \left(1 - \sum_{k=0}^{\tau-1} x_{t-k} \right), \quad (3.2)$$

where the parameter a reflects the infection rate. Similar to the model of Cooke *et al.* (1977; Girvan *et al.* 2002), the map in equation (3.2) has a Hopf bifurcation (or more exactly Neimark bifurcation) curve that divides the $\tau - a$ parameter plane into two. The region in parameter space above the curve in figure 3 (numerically obtained) characterizes oscillatory behaviour, while the region below the curve characterizes a stable fixed point. The Hopf curve itself is the point at which the model passes through a Hopf bifurcation.

Now consider two coupled SIRS models ($s_i^{1,2}, x_i^{1,2}$) given by equation (3.2). Typical coupling schemes might be as follows.

- (i) Infective coupling type 1:

$$x_{t+1}^{1,2} = (1 - e)ax_i^{1,2}s_i^{1,2} + eax_t^{2,1}s_t^{2,1}. \quad (3.3)$$

- (ii) Infective coupling type 2:

$$x_{t+1}^{1,2} = a(x_t^{1,2} + ex_t^{2,1})s_t^{1,2}. \quad (3.4)$$

- (iii) Diffusive coupling:

$$x_{t+1}^{1,2} = ax_i^{1,2}s_i^{1,2} + e(x_t^{2,1} - x_t^{1,2}). \quad (3.5)$$

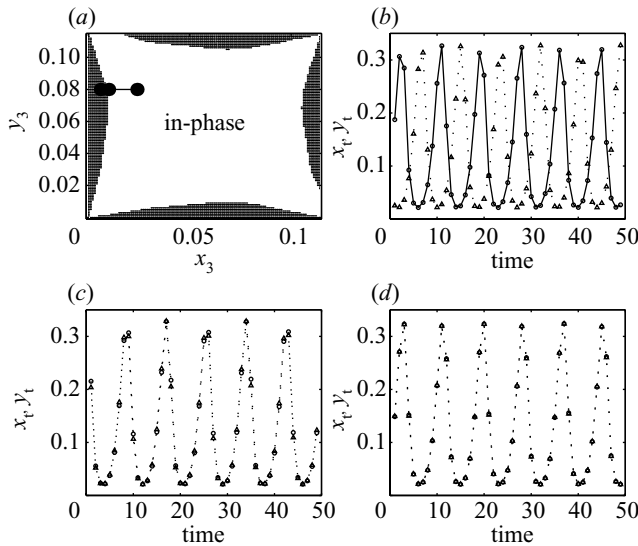


Figure 4. Infective type 1 coupling with parameters $\tau = 4$, $a = 2.4$, $e = 0.001$ the attractive basins of in-phase and antiphase (hatched) solution. (a) x_3 (horizontal axis) and y_3 (vertical axis); other initial values are set zero. The three marked filled circles from left to right correspond to the time series of antiphase (b), in-phase (c) and in-phase (d).

Using parameters $\tau = 4$ and $a = 2.4$, the discrete SIRS model oscillates with mean period 2τ as in figure 4. With weak infective coupling (type 1 $e = 0.0005\text{--}0.006$), their oscillations can be observed to either synchronize in-phase or antiphase depending on initial conditions. Thus, the two types of synchronization behaviour coexist for the same model parameters. Figure 4a plots the basins of attraction for in-phase and antiphase synchronization based on initial conditions for x_3, y_3 , assuming that $x_0^i = x_1^i = x_2^i = y_0^i = y_1^i = y_2^i = 0$. For $e > 0.006$ only pure in-phase synchronization is attained. (Note that if the coupling is extremely weak ($e < 0.0005$), the models are unable to form stable synchronization.)

For weak diffusive and infective type 2 coupling, the emerging pattern is different. In-phase and antiphase synchronization were never found to coexist. Pure stable antiphase oscillations were found over a larger coupling regime ($e = 0.0001\text{--}0.05$), while in-phase synchronization only occurs at much larger coupling levels ($e > 0.05$). In other words, these discrete-time SIRS models qualitatively match the behaviour of the random network simulation model.

4. WHY DO EPIDEMICS SYNCHRONIZE IN- AND OUT-OF-PHASE?

To gain deeper insights into the synchronization dynamics, consider first two weakly coupled continuous time oscillators of very general form

$$\dot{\mathbf{X}}_{1,2} = F(\mathbf{X}_{1,2}) + \varepsilon D(\mathbf{X}_{2,1} - \gamma \mathbf{X}_{1,2}), \tag{4.1}$$

where $\mathbf{X}_{1,2}$ are two m -dimensional vectors, each oscillator being characterized by its own m -variables, and F defines the system of equations describing each oscillator. (Namely, $\mathbf{X}_{1,2} \in R^m$, $F: R^m \rightarrow R^m$.) When $\varepsilon = 0$, the individual oscillators have stable limit cycle solutions of period $2\pi/\omega_0$. D is an $m \times m$ coupling matrix, and coupling

is very weak with $\varepsilon \ll 1$. When $\gamma = 1$ the coupling is diffusive and when $\gamma = 0$ the coupling is termed direct. Let $\omega_{1,2} = \omega_0 + O(\varepsilon)$ be the frequency of the limit cycles of two oscillators in the presence of coupling. Ermentrout & Kopell (1984) have shown that there is a two-dimensional submanifold of R^{2m} which is attracting and invariant. This manifold is a two-dimensional torus T^2 . These authors have also proved that the variables θ_1 and θ_2 may be chosen on the torus so that, if $\phi = \theta_2 - \theta_1$, then the equations for θ_1 and ϕ can be well approximated by

$$\begin{aligned} \dot{\theta}_1 &= \omega_1 + \varepsilon H(\phi), \\ \dot{\phi} &= \varepsilon[\omega_2 - \omega_1 + H(-\phi) - H(\phi)]. \end{aligned} \tag{4.2}$$

Here, $H(\phi)$ is a 2π -periodic function of the phase difference ϕ , and depends on the form of the coupling D and on the dynamics of the oscillators in the neighbourhood of the limit cycle.

More explicitly, consider the following specific model with $m = 2$ and

$$\mathbf{X} = \begin{pmatrix} x \\ y \end{pmatrix}, D = \begin{pmatrix} d_1 & d_2 \\ d_3 & d_4 \end{pmatrix} F \begin{pmatrix} x \\ y \end{pmatrix} = \begin{pmatrix} \lambda & -\omega \\ \omega & \lambda \end{pmatrix} \begin{pmatrix} x \\ y \end{pmatrix},$$

where $\lambda = 1 - (x^2 + y^2)$, $\omega = \omega_0 + q(1 - x^2 - y^2)$. The parameter q is referred to as shear and quantifies the effect of amplitude of the oscillation on the frequency. This is the classical $\lambda - \omega$ system that typifies dynamics close to a Hopf bifurcation. The parameters d_2 and d_3 represent what is referred to as ‘cross coupling’ between the two systems (Aronson *et al.* 1990).

The system is much easier to work with in polar coordinates ($x = r \cos \theta$, $y = r \sin \theta$), and may be written equivalently as

$$\left. \begin{aligned} \dot{r} &= r(1 - r^2) \\ \dot{\theta} &= \omega_0 + q(1 - r^2) \end{aligned} \right\}. \tag{4.3}$$

This makes clear the way in which the amplitude dynamics r affects the phase dynamics θ via the shear parameter q . On the limit cycle, the radius $r = 1$ and the shear term $q(1 - r^2) = 0$. If at any time the radius $r > 1$, then $\dot{\theta}$ is reduced by the negative shear term $q(1 - r^2)$. Conversely, if $r < 1$ then $\dot{\theta}$ is increased by a corresponding positive shear term. With the introduction of diffusive coupling as in equation (4.1), a direct calculation shows that $H(\phi)$ of equation (4.2) is

$$\begin{aligned} H(\phi) &= \frac{1}{2}[(d_3 - d_2) - q(d_1 + d_4)](\cos \phi - \gamma) \\ &+ \frac{1}{2}[(d_1 + d_4) - q(d_2 - d_3)] \sin \phi. \end{aligned} \tag{4.4}$$

The equation governing the dynamics of the phase difference between the two oscillators may therefore be approximated, using equation (4.2), as

$$\dot{\phi} = \varepsilon[\omega_2 - \omega_1 - (d_1 + d_4) + q(d_2 - d_3)] \sin \phi. \tag{4.5}$$

Assuming $\omega_1 = \omega_2$, this equation implies that there is a stable antiphase solution $\phi = \pi$ if (Ermentrout & Kopell 1984)

$$q(d_2 - d_3) > d_1 + d_4. \tag{4.6}$$

Otherwise the in-phase solution $\phi = 0$ is stable. This important condition was first pointed out in Ermentrout &

Kopell (1984). One sees this easily by plotting $\dot{\phi}$ versus ϕ in the phase plane and examining the equilibrium points where $\dot{\phi} = 0$. Criterion (4.6) makes it clear that both cross coupling ($d_2 > 0$) and shear ($q > 0$) are necessary conditions for stable antiphase synchronization.

To shed further light on the relation between shear and antiphase in time-discrete systems, we consider the following coupled two-dimensional Hopf-bifurcation map system (Lloyd 1995),

$$\mathbf{X}'_{1,2} = G(\mathbf{X}_{1,2}) + D(\mathbf{X}_{2,1} - \mathbf{X}_{1,2}), \quad (4.7)$$

where

$$\mathbf{X}_{1,2} = \begin{pmatrix} x_{1,2} \\ y_{1,2} \end{pmatrix}, D = \begin{pmatrix} d_1 & d_2 \\ d_3 & d_4 \end{pmatrix}, \quad (4.8)$$

$$G \begin{pmatrix} x \\ y \end{pmatrix} = \{\lambda - (x^2 + y^2)\} \begin{pmatrix} \cos \alpha & -\sin \alpha \\ \sin \alpha & \cos \alpha \end{pmatrix} \begin{pmatrix} x \\ y \end{pmatrix}. \quad (4.9)$$

Here, we use the common shorthand mapping notation whereby $\mathbf{X}' = \mathbf{X}_{t+1}$ while $\mathbf{X} = \mathbf{X}_t$. With α fixed, λ acts as a bifurcation parameter. The origin is always a fixed point and the Jacobian has eigenvalues $\lambda(\cos \alpha \pm i \sin \alpha)$. Both eigenvalues have modulus $|\lambda|$ so that the unit circle is crossed as λ is increased beyond unity. When $\lambda < 1$ the origin is stable, and when λ passes through $\lambda = 1$ a Hopf bifurcation occurs and oscillations ensue.

Changing to polar coordinates (r, θ) the map G becomes

$$\begin{aligned} r_{t+1} &= \lambda r_t - r_t^3 \\ \theta_{t+1} &= \theta_t + \alpha \end{aligned} \quad (4.10)$$

As the phase dynamics are completely unaffected by the amplitude r , the system has no shear. In the formulation of equation (4.3), this means $q = 0$. Hence, by condition (4.6) the coupled system only exhibits in-phase synchronization. Indeed, numerical simulations find only in-phase synchronization between two such coupled map systems when $\lambda > 1$ and α is not too large (e.g. $\alpha < 1$).

Shear can be introduced by setting α in equations (4.8) and (4.9) as

$$\alpha = \omega_0 + q(\lambda - 1 - r_t^2). \quad (4.11)$$

This takes into account that the radius of the oscillation on the limit cycle is given by $r^2 = \lambda - 1$, as found from equation (4.10). When ω_0 is relatively small (e.g. $\omega_0 \leq 0.1$), the synchronization behaviour of the coupled discrete model system closely resembles that of the time continuous system above. Figure 5 plots regimes of in-phase and antiphase synchronization as a function of d_1 and d_2 ($d_3 = d_4 = 0.001$, $q = 1$, $\omega_0 = 0.1$, $\lambda = 1.01$). The *plane* in figure 5 corresponds to $q(d_2 - d_3) = d_1 + d_4$ which according to criterion (4.6) and the theory for the continuous time case, should divide the $d_1 - d_2$ plane into pure in-phase and pure antiphase synchronization regions. As can be seen, the theoretical predictions of the continuous time model extends to the discrete-time model well.

However, when ω_0 is relatively large ($\omega_0 = 0.5-1.5$) we find that antiphase synchronization results often when in-phase is expected. For example, figure 6 plots synchronization regimes as a function of shear q and mean frequency (rotation number) ω_0 (when $d_1 = 0.005$, $d_2 = d_3 = d_4 = 0$). Under these parameters, criterion (4.6) would predict for

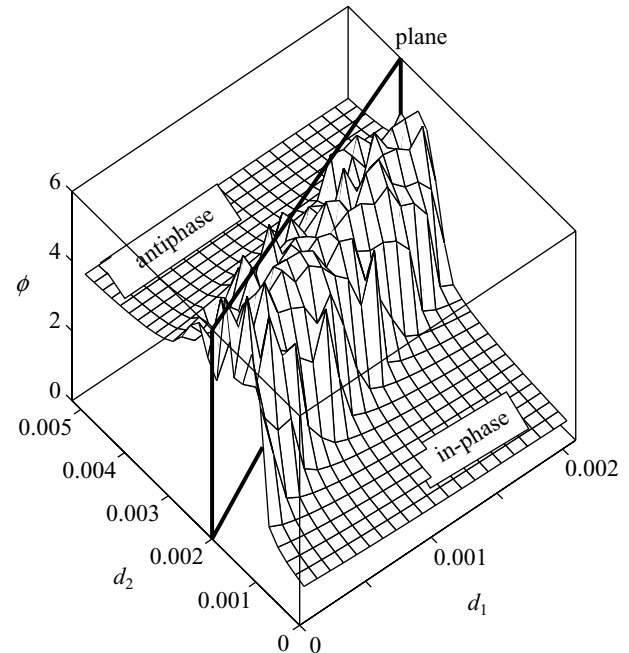


Figure 5. Average phase difference ϕ as a function of d_1 and d_2 for two weakly coupled Hopf-bifurcation maps (equation (4.7)). Parameters $d_3 = d_4 = 0.001$, $q = 1$, $\omega_0 = 0.1$, $\lambda = 1.01$. The *plane* corresponds to $q(d_2 - d_3) = d_1 + d_4$ which divides the $d_1 - d_2$ plane into in-phase and antiphase regions.

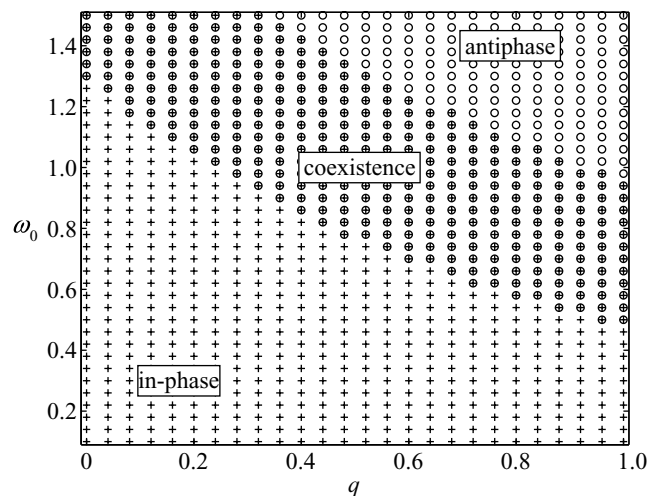


Figure 6. Two identical weakly coupled Hopf-bifurcation maps (4.2), with $\lambda = 1.01$, $d_1 = 0.005$, $d_2 = d_3 = d_4 = 0$. Mean frequency ω_0 versus shear q . Each point corresponds to 100 simulations each with different initial conditions. The $q - \omega_0$ parameter space divides into three regions: only in-phase (+), only antiphase (open circles) and coexistence of both (circles with plus signs).

continuous time systems (i.e. $\omega_0 \rightarrow 0$) the establishment of in-phase synchronization only. Instead, as figure 6 shows, there are large parameter regions of pure in-phase, antiphase and the coexistence of both in-phase and antiphase synchronization. Presumably the discreteness of the mapping (which becomes more acute the larger is ω_0) is the cause of the divergence from criteria (4.6), known to be accurate for the continuous time model.

5. IMPLICATIONS OF THE THEORY FOR EPIDEMIC MODELS

The synchronization results in § 4 should be generic to all coupled model oscillators in the vicinity of a Hopf bifurcation. They are thus relevant to the epidemic models discussed in § 3 whose oscillations are induced through a Hopf bifurcation. Shear appears to be one of the important requirements for antiphase synchronization. But we have not yet checked whether the epidemic models studied earlier have this property. Some idea can be gained through considering the following delayed regulation population model (Aronson *et al.* 1982):

$$\left. \begin{aligned} x_{t+1} &= ax_t(1 - y_t) \\ y_{t+1} &= x_t \end{aligned} \right\} \tag{5.1}$$

with the single parameter a . The model is closely related to the epidemic equations (3.2) only that it has fewer time delayed elements. This is more easily seen by rewriting equation (5.1) as

$$x_{t+1} = ax_t(1 - x_{t-1}). \tag{5.2}$$

The model has the fixed point at $x^* = y^* = (a - 1)/a$, which is locally stable for $1 < a \leq 2$. As a passes through the value 2, this fixed point loses stability and spawns an attracting invariant circle via a Hopf bifurcation. Shifting the equilibrium to the origin through the parameter change $u_t = x_t - x^*$, $v_t = y_t - y^*$ gives

$$\left. \begin{aligned} u_{t+1} &= u_t - (a - 1)v_t - au_tv_t \\ v_{t+1} &= u_t \end{aligned} \right\} \tag{5.3}$$

If we set $(u_t, v_t) = r_t(\cos \theta_t, \sin \theta_t)$, then

$$\begin{aligned} \theta_{t+1} &= \arctan\left(\frac{v_{t+1}}{u_{t+1}}\right) \\ &= \arctan((1 - (a - 1)\tan(\theta_t) - ar_t \sin \theta_t)^{-1}) \\ &= f(\theta_t, r_t). \end{aligned} \tag{5.4}$$

This makes it clear that the amplitude r_t directly affects θ_{t+1} , and the system thus has shear. The mean frequency is

$$\omega_0 = \arctan\left(\frac{\text{Im}\lambda_{\pm}}{\text{Re}\lambda_{\pm}}\right) \approx \pm 1.0472, \tag{5.5}$$

where $\lambda_{\pm} = (1 \pm \sqrt{4a - 5})/2$ are the eigenvalues of the delayed regulation map with $a = 2.01$. Owing to the shear identified above and the relatively high mean frequency, it is not surprising that this epidemic-like model exhibits antiphase with weak coupling, as numerical simulations show.

Returning now to the full SIRS equation (3.2), we note that model itself is high dimensional owing to the presence of time delays. However, by a theorem of Ermentrout & Kopell (1984) (see also Aronson *et al.* 1990), near the Hopf bifurcation the model can be approximated by a two-dimensional system with only phase (θ) and amplitude (r) variables. There are several practical methods to decompose the phase and amplitude variables given a time-series record of a single variable, say the infected population $x(t)$. The peak-to-peak outbreak statistics (see Blasius & Stone 2000) is one common method since this

gives information on the speed of the phase evolution and also the amplitude of the outbreaks. Although more difficult to implement, we prefer to make use of the Hilbert transform (Pikovsky *et al.* 2001) for obtaining the phase and amplitude decomposition, a powerful methodology specifically designed for this task. We briefly give the details of the method for completeness, but the less mathematically inclined reader will lose nothing by moving straight to the results given in the next paragraph. The Hilbert transform of the time series $H(x)$ is defined as

$$H[x(t)] = \text{PV}\left(\frac{1}{\pi} \int_{-\infty}^{\infty} \frac{x(\tau)}{t - \tau} d\tau\right), \tag{5.6}$$

where PV stands for the Cauchy principal value of the integral. The phase and amplitude are then given by

$$r^2(t) = x^2(t) + H^2[x(t)], \quad \theta(t) = \arctan\left(\frac{H[x(t)]}{x(t)}\right). \tag{5.7}$$

Using the Hilbert transform we can analyse discrete time-series to obtain the relationship between $\Delta\theta = \theta(t + 1) - \theta(t)$ and $r^2(t)$. For example, for the case of equations (4.10) and (4.11), it would be expected that $\Delta\theta \approx -qr^2(t)$, where q is the coefficient of shear. We used time-series generated by system (4.10, 4.11) under different levels of shear q . By plotting $\Delta\theta$ versus q it is possible to estimate q by calculating the slope of the linearly least squares fit to the points in the plane.

The results for $q = 0$ and $q = 2$ in system (4.10, 4.11) are given in figure 7a,b, respectively. The estimates of q ($\hat{q} = 0.05$, $\hat{q} = 2.1$) match the true parameter values accurately. An estimation of shear of $q = 10$ is found for system (3.2) (with $\tau = 4$) as seen from figure 7c. The estimation for shear in the epidemic oscillations of the random network is found to be $q = 2.5$ as seen in figure 7d. Shear is estimated for real epidemic data of London and Birmingham and, as figure 7e,f shows, is $q \approx 4.9$ and $q \approx 10$, respectively. Thus, shear, which is a prerequisite for antiphase synchronization, is apparent in model and empirical epidemiological datasets.

6. CONCLUSION

Based on empirical data of measles incidence patterns over England and Wales and based on results of simulation models, Grenfell *et al.* (2001) proposed two important hypotheses concerning the spatio-temporal synchronization of epidemics.

- (i) Strong coupling of large [city] centres ‘should generate highly synchronized dynamics ... as a result of nonlinear phase locking of seasonally forced oscillations’.
- (ii) Alternatively, ‘weakly coupled or distant centres should have a stronger tendency than nearer towns to move onto the ‘opposite’ [antiphase] biennial attractor from the main conurbation’.

The theoretical results outlined here provide strong support for their observations. It is interesting to note that the results we present broadly correspond to those of the simulation models of Grenfell *et al.* (2001) even though the latter were seasonally forced. It remains a challenge

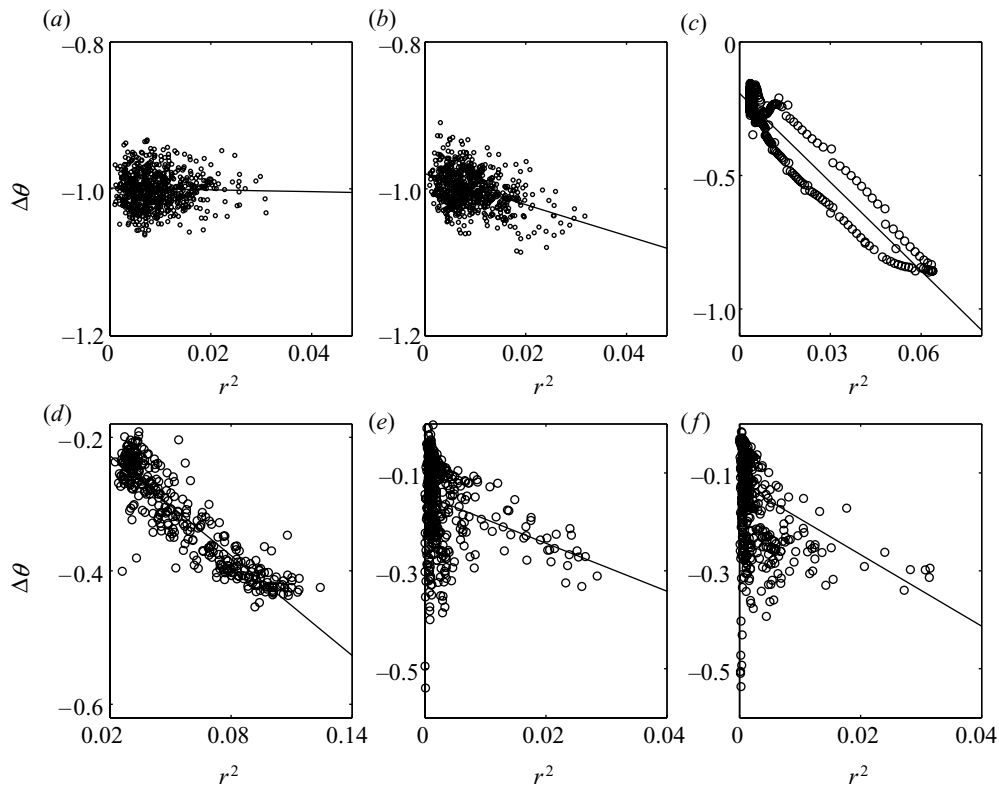


Figure 7. Estimation of shear by the Hilbert transform method: (a) equations (4.10) and (4.11) with $q=0$ have shear estimate $\hat{q}=0.05$; (b) equations (4.10) and (4.11) with $q=2$ have shear estimate $\hat{q}=2.1$; (c) SIRS epidemic model equation (3.2) has shear estimate $\hat{q}=10$; (d) random network epidemic model has shear estimate $\hat{q}=2.5$; (e) measles cases from London (1944–1966) have shear estimate $\hat{q}=4.9$; (f) measles cases from Birmingham (1944–1966) have shear estimate $\hat{q}=10$.

for the future to extend the theory to the seasonally forced case. However, the essential ingredients controlling the actual type of synchronization appear to rely on the shear of the dynamics and, as Grenfell *et al.* (2001) find, the strength of the coupling. We expect the findings outlined here to be mirrored in seasonally forced models, as there is some genericity underlying the synchronization dynamics of coupled oscillators. In actual fact, Grenfell *et al.* (2001) take the above hypotheses further and show that there is a huge amount of systematic phase variation superimposed on the phase locked synchrony. This indicates travelling waves, possibly arising from ‘forest fire’-like dynamics wherein sparks from larger cities initiate epidemics in small ones, but with a lag. We are currently exploring the connection between travelling waves and synchrony from a theoretical perspective in these epidemic models.

The implications of epidemic synchronization is also an area that needs further research (Stone *et al.* 2002). Existing theory suggests that it is a feature that may be taken advantage of when designing vaccination policies (Earn *et al.* 2000). For example, pulse vaccination (Shulgin *et al.* 1998; Earn *et al.* 1998) can enhance in-phase spatial synchronization if applied regularly and simultaneously across all suburbs at periodic time intervals. When oscillating infection levels reach minima at the same time in all suburbs, this enhances the probability of global fade-out and extinction of the disease. By contrast, antiphase synchronization tends to promote endemic infection owing to what is termed the ‘rescue effect’ (Gotelli 1998).

Although the disease in one population may reach extinction, it can nevertheless reappear from an antiphase supply of immigrants in another suburb. Epidemic outbreaks bounce in turn from one suburb to the other as seen in figure 1b for Cambridge and Norwich, reducing the chance of disease extinction. Thus, the spatio-temporal synchronization dynamics of epidemics has important practical consequences.

The authors are grateful for the support of the James S. McDonnell Foundation. The data displayed in figure 1 were kindly supplied by Professor B. T. Grenfell.

REFERENCES

- Anderson, R. M. & May, R. M. 1991 *Infectious diseases of humans: dynamics and control*. Oxford University Press.
- Anderson, R. M., Grenfell, B. T. & May, R. M. 1984 Oscillatory fluctuations in the incidence of infectious disease and the impact of vaccination: time series analysis. *J. Hyg. Camb.* **93**, 587–608.
- Aronson, D. G., Chory, M. V., Hall, G. R. & McGehee, R. P. 1982 Bifurcations from an invariant circle for two-parameter families of maps of the plane: a computer-assisted study. *Commun. Math. Phys.* **83**, 304–354.
- Aronson, D. G., Ermentrout, G. B. & Kopell, N. 1990 Amplitude response of coupled oscillators. *Physica D* **41**, 403–449.
- Blasius, B. & Stone, L. 2000 Chaos and phase synchronization in ecological systems. *Int. J. Bifur. Chaos* **10**, 2361–2380.
- Cooke, K. L., Calef, D. F. & Level, E. V. 1977 *Nonlinear systems and its application*, pp. 73–93. New York: Academic.

- Earn, D. J. D., Rohani, P. & Grenfell, B. T. 1998 Persistence, chaos and synchrony in ecology and epidemiology. *Proc. R. Soc. Lond. B* **265**, 7–10. (DOI 10.1098/rspb.1998.0256.)
- Earn, D. J. D., Levin, S. A. & Rohani, P. 2000 Coherence and conservation. *Science* **290**, 1360–1364.
- Ermentrout, G. B. & Kopell, N. 1984 Frequency plateaus in a chain of weakly coupled oscillators. *SIAM J. Math. Anal.* **15**, 215–237.
- Girvan, M., Callaway, D. S., Newman, M. E. J. & Strogatz, S. H. 2002 A simple model of epidemic with pathogen mutation. *Phys. Rev. E* **65**, 031 915.
- Gotelli, N. J. 1998 *A primer of ecology*. Sunderland, MA: Sinauer.
- Grenfell, B. T., Bjørnstad, O. N. & Kappey, J. 2001 Travelling waves and spatial hierarchies in measles epidemics. *Nature* **414**, 716–723.
- Hethcote, H. W. & Levin, S. A. 1989 Periodicity in epidemiological models. In *Applied mathematical ecology* (ed. S. A. Levin, T. G. Hallam & L. J. Gross), pp. 193–211. Berlin: Springer.
- Karlen, A. 1995 *Man and microbes: disease and plagues in history and modern times*. New York: Simon and Schuster.
- Keeling, M. H. & Rohani, P. 2002 Estimating spatial coupling in epidemiological systems: a mechanistic approach. *Ecol. Lett.* **5**, 20–29.
- Kuperman, M. & Abramson, G. 2001 Small world effect in an epidemiological model. *Phys. Rev. Lett.* **86**, 2909–2912.
- Lloyd, A. L. 1995 The coupled logistic map: a simple model for the effects of spatial heterogeneity on population dynamics. *J. Theor. Biol.* **179**, 217–230.
- Lloyd, A. L. & May, R. M. 1996 Spatial heterogeneity in epidemic models. *J. Theor. Biol.* **86**, 1–11.
- Pikovsky, A., Rosenblum, M. & Kurths, J. 2001 *Synchronization: a universal concept in nonlinear sciences*. Cambridge University Press.
- Rohani, P., Keeling, M. J. & Grenfell, B. T. 2002 The interplay between determinism and stochasticity in childhood diseases. *Am. Nat.* **159**, 469–481.
- Shulgin, B., Stone, L. & Agur, Z. 1998 Pulse vaccination strategy in the SIR epidemic model. *Bull. Math. Biol.* **60**, 1123–1148.
- Stone, L., Olinky, R., Blasius, B., Huppert, A. & Cazelles, B. 2002 Complex synchronization phenomena in ecological systems. In *Experimental chaos, American Institute of Physics Conference Proceedings 622, Melville, New York* (ed. S. Boccaletti, B. J. Gluckman, J. Kurths, L. M. Pecora & M. L. Spano), pp. 476–487. Melville, New York: American Institute of Physics.

As this paper exceeds the maximum length normally permitted, the authors have agreed to contribute to production costs.